Transition from the exhibition to the nonexhibition of negative differential thermal resistance in the two-segment Frenkel-Kontorova model

Zhi-Gang Shao,[1] Lei Yang,[1,2,*] Ho-Kei Chan,[1] and Bambi Hu[1,3]

[1]*Department of Physics, Centre for Nonlinear Studies, The Beijing-Hong Kong-Singapore Joint Centre for Nonlinear and Complex Systems (Hong Kong), Hong Kong Baptist University, Kowloon Tong, Hong Kong, China*

[2]*Institute of Modern Physics, Chinese Academy of Sciences, and Department of Physics, Lanzhou University, Lanzhou, 730000 China*

[3]*Department of Physics, University of Houston, Houston, Texas 77204-5005, USA*

(Received 5 January 2009; revised manuscript received 26 February 2009; published 22 June 2009)

An extensive study of the one-dimensional two-segment Frenkel-Kontorova (FK) model reveals a transition from the counterintuitive existence to the ordinary nonexistence of a negative-differential-thermal-resistance (NDTR) regime, when the system size or the intersegment coupling constant increases to a critical value. A "phase" diagram which depicts the relevant conditions for the exhibition of NDTR was obtained. In the existence of a NDTR regime, the link at the segment interface is weak and therefore the corresponding exhibition of NDTR can be explained in terms of effective phonon-band shifts. In the case where such a regime does not exist, the theory of phonon-band mismatch is not applicable due to sufficiently strong coupling between the FK segments. The findings suggest that the behavior of a thermal transistor will depend critically on the properties of the interface and the system size.

DOI: 10.1103/PhysRevE.79.061119 PACS number(s): 05.60.−k, 44.10.+i, 05.70.Ln, 07.20.−n

I. INTRODUCTION

When a thermodynamic force X is applied to a system, the system may exhibit a flux Y of a certain attribute and the system's resistance to the flux is $R=X/Y>0$. In some cases, Y decreases counterintuitively with increasing X and the state of negative differential resistance (NDR) occurs. In the case of electrical conduction, the state of NDR occurs during the operation of a number of semiconductor devices, for example the tunnel diode [1]. In the case of heat conduction, the concept of negative differential thermal resistance (NDTR) has emerged from recent efforts to design and build the thermal counterparts of present-day electrical devices. One possibility for the exhibition of NDTR lies in a two-layer system: the phonon band of each layer will shift with any change in the temperature of that layer. If the temperature difference between the layers is enlarged but, due to the phonon-band shifts of the individual layers, the degree of phonon-band overlap between the layers decreases, the heat flux across the layers will drop and the phenomenon of NDTR will occur.

In recent years, much attention has been paid to the effects of nonlinearity on thermal transport in low-dimensional systems [2,3]. Recent theoretical studies have shown that some low-dimensional nonlinear systems exhibit thermal rectification [4–15] and some even exhibit NDTR [13–15]. Designs of thermal transistors, thermal logic gates, and thermal-memory devices based on low-dimensional lattice models have recently been proposed [13,16], and their operational principles are fundamentally based on the concept of NDTR. It can be seen that the concept of NDTR is and will remain an important ingredient in the designing of a variety of next-generation thermal devices, and therefore a fundamental understanding of the physical mechanism of NDTR is urgently needed.

*Corresponding author.

II. MODEL AND METHOD

The Frenkel-Kontorova (FK) model [17–20] has found a wide range of applications in condensed-matter systems, from adsorbed monolayers, Josephson junctions, charge-density waves, magnetic spirals, tribology, transport properties of vortices in easy-flow channels, to strain-mediated interaction of vacancy lines in pseudomorphic adsorbate systems. This paper reports a NDTR study of the one-dimensional two-segment FK model, which consists of two FK segments connected by a harmonic spring; the coupling constant of the intersegment harmonic spring is here denoted as k_{int}. The size of the left segment and that of the right segment are here denoted as N_L and N_R, respectively. The total Hamiltonian of the model is

$$H = H_L + H_R + H_{int}, \tag{1}$$

where H_L and H_R are the Hamiltonians of the left and the right segment, respectively, and H_{int} is the Hamiltonian of the segment interface. The Hamiltonian of each segment is given by

$$H_W = \sum_{i=1}^{N_W} \left[\frac{p_{W,i}^2}{2m} + \frac{k_W}{2}(x_{W,i} - x_{W,i-1})^2 - \frac{V_W}{(2\pi)^2}\cos 2\pi x_{W,i} \right], \tag{2}$$

where $W=L$ or R, $x_{W,i}$ is the ith particle's displacement from its equilibrium position, $p_{W,i}$ is the ith particle's conjugate momentum, k_W is the strength of the interparticle potential, and V_W is the strength of the external potential from the FK lattice. It follows that, at the segment interface, $H_{int} = \frac{k_{int}}{2}(x_{L,N_L} - x_{R,N_R})^2$.

Nonequilibrium molecular-dynamics simulation is used. The Langevin heat baths are taken and the equation of motion is integrated by using a fourth-order Runge-Kutta algorithm. In the simulations, the parameter values $m=1$, $V_L=5$, $V_R=1$, $K_L=1$, and $K_R=0.2$ were employed, the parameters

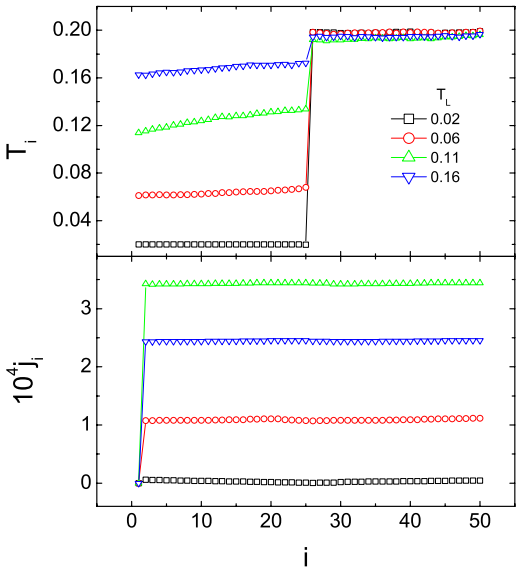

FIG. 1. (Color online) The local temperature T_i and local flux j_i as functions of the position i for various T_L with $k_{int}=0.05$ and $N=25$.

are the same as the ones in Ref. [13], and the parameters under study were k_{int} and a system size of $N=N_L=N_R$. Since the segments have different parameter values, the model under study could generally exhibit asymmetric heat conduction. The boundary conditions were fixed at $x_{L,0}=x_{R,0}=0$, with the particles at the left and the right boundary connected to individual Langevin heat baths at temperatures T_L and T_R, respectively. The equations of motion of particles are as follows:

$$\ddot{x}_{W,1} = -\frac{\partial H}{\partial x_{W,1}} - \lambda_W \dot{x}_{W,1} + \xi_W,$$

$$\ddot{x}_{W,i} = -\frac{\partial H}{\partial x_{W,i}}, \quad i = 2, \cdots, N_W, \tag{3}$$

where $W=L$ or R, and $\lambda_W=0.1$ is the coupling constant (damping constant) between the Langevin heat bath and the chain. ξ_W is independent Wiener processes with zero mean, variance $2\lambda_W T_W$. In the bulk of the model, the local temperature and local heat flux were defined as $T_i=m\langle \dot{x}_i^2 \rangle$ and $j_i=k_i\langle \dot{x}_i(x_i-x_{i-1})\rangle$, respectively. Figure 1 shows the local temperature T_i and local flux j_i as functions of the position i for various T_L with $k_{int}=0.05$ and $N=25$. To calculate the mean values, the time mean and random seed mean are taken. The noise is white noise and the damping constant of Langevin heat bath $\lambda=0.1$. After the system reaches a stationary state, j_i is independent of site position i, so the flux can be defined as steady-state heat flux J. To obtain a steady-state heat flux J and a steady-state temperature profile, each simulation was performed long enough with about 10^9 iterations. For each set of chosen values of k_{int} and N, the steady-state heat flux J was investigated as a function of the temperature T_L of the left boundary while the temperature of the right boundary was fixed at $T_R=0.2$. It follows that, in the plot of J against T_L, the regime of positive slope is the regime of NDTR.

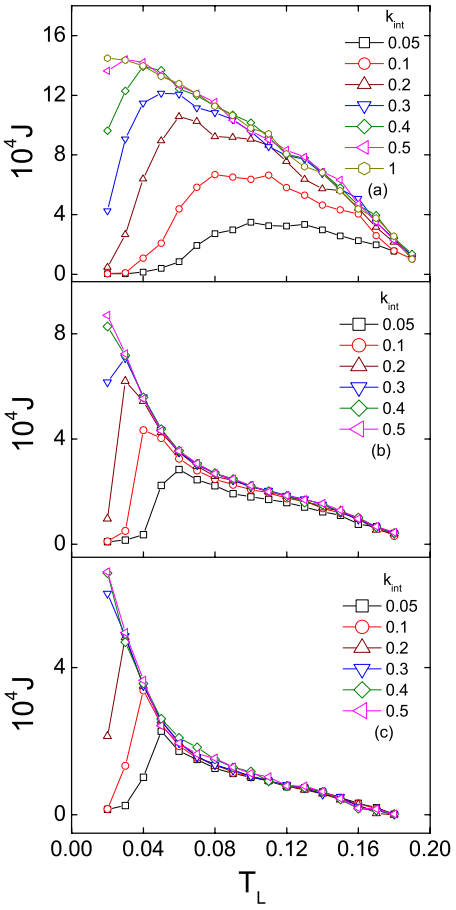

FIG. 2. (Color online) Heat flux as a function of the temperature T_L of the left boundary for various values of k_{int}, at a system size of (a) $N=25$, (b) $N=150$, and (c) $N=250$.

The temperature used in our numerical simulation is dimensionless. It is connected with the true temperature T_r through the following relation [7,21]: $T_r=\frac{m\omega_0^2 b^2}{k_B}T$, where m is the mass of the particle and b is the period of external potential. ω_0 is the vibration frequency. k_B is the Boltzman constant. For the typical values of atoms, we have $T_r \sim (10^2-10^3)T$ [7,21], which means that the room temperature corresponds to the dimensionless temperature $T \sim (0.1-1)$.

III. TRANSITION

Figure 2 depicts how the coupling constant k_{int} affects the temperature dependence of the heat flux J for a system size of $N=25$, 150, and 250. For the purpose of comparison, it is worth pointing our that, in Fig. 2(a), the case of $N=25$ and $k_{int}=0.05$ is one that is also presented in Fig. 3(c) in Ref. [13]. For each value of the system size, the heat flux J is presented as a function of the temperature T_L of the left boundary for different values of k_{int} and, as explained above, the regime of positive slope is the regime of NDTR. As shown in Fig. 2, for each value of the system size, the regime of NDTR diminishes for increasing k_{int} until it vanishes at a critical coupling constant $k_{int}=k_c$. It can also be seen that

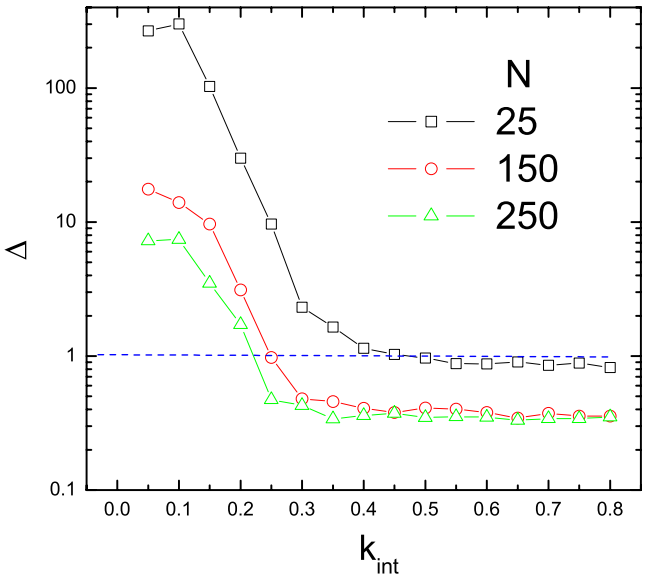

FIG. 3. (Color online) The thermal-diode gain Δ as a function of the coupling constant k_{int} for a system size of N=25, 150, and 250. The dashed blue line indicates the case of Δ=1.

there is a general decrease in k_c as the system size increases from N=25 to N=250.

It was found that the transition from the exhibition to the nonexhibition of NDTR coincides with a thermal-diode gain of unity. The thermal-diode gain of the system is defined as $\Delta=|J_+/J_-|$, where J_+ is the heat current from left to right for T_L=0.2 and T_R=0.02 and J_- the heat current from right to left for T_R=0.2 and T_L=0.02. Figure 3 depicts the thermal-diode gain Δ as a function of the coupling constant k_{int} for a system size of N=25, 150, and 250. The dashed blue line indicates the case of Δ=1, i.e., $J_+=J_-$. As the coupling constant k_{int} increases, the thermal-diode gain Δ decreases. A comparison with Fig. 2 reveals that the case of Δ=1 coincides with the vanishing of the NDTR regime at the critical coupling constant k_c.

Figure 4 depicts how the system size N affects the temperature dependence of the heat flux J for a coupling constant of k_{int}=0.05, 0.3, and 0.5. For the purpose of comparison, it is again worth pointing out that, in Fig. 4(a), the cases of k_{int}=0.05 and N=25 and 50 are ones that are also presented in Fig. 3(c) in Ref. [13]. As shown in Fig. 4, for each value of the coupling constant, the regime of NDTR diminishes for increasing system size until it vanishes at a critical system size N_c. It can also be seen that there is a general decrease in N_c as the coupling constant increases from k_{int} =0.05 to k_{int}=0.5.

Figure 5 depicts the thermal-diode gain Δ as a function of the system size N for a coupling constant of k_{int}=0.05, 0.3, and 0.5. The dashed blue line indicates the case of Δ=1. As the system size N increases, the thermal-diode gain Δ decreases until it stays at a constant value; This can be understood by regarding the segment interface as an "impurity;" As the system size increases, the relative importance of the impurity decreases and hence the thermal-diode gain decreases [9]. A comparison with Fig. 4 also reveals that the case of Δ=1 coincides with the vanishing of the NDTR regime at the critical system size N_c.

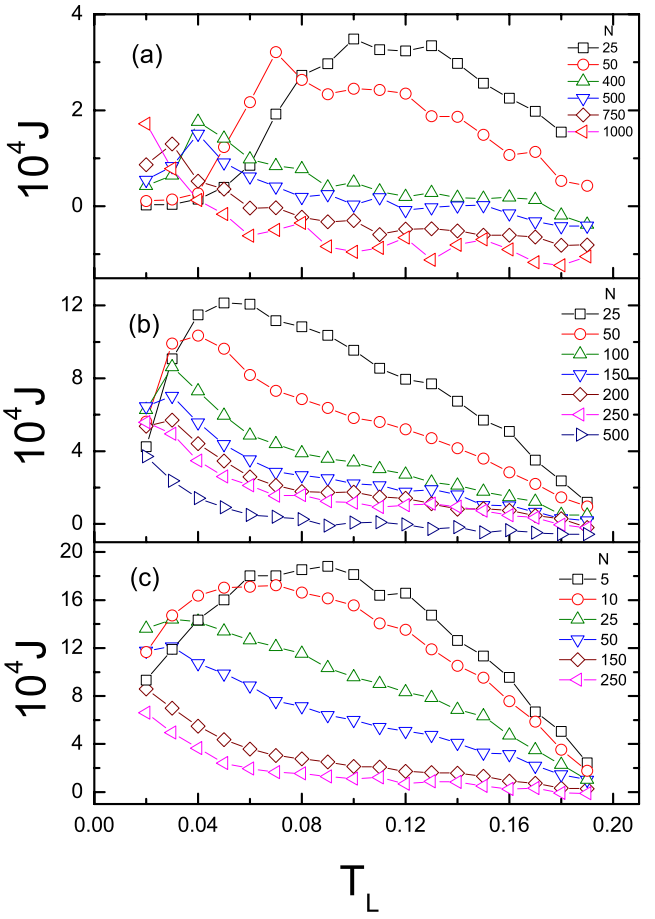

FIG. 4. (Color online) Heat flux as a function of the temperature T_L of the left boundary for various values of N, with a coupling constant of (a) k_{int}=0.05, (b) k_{int}=0.3, and (c) k_{int}=0.5.

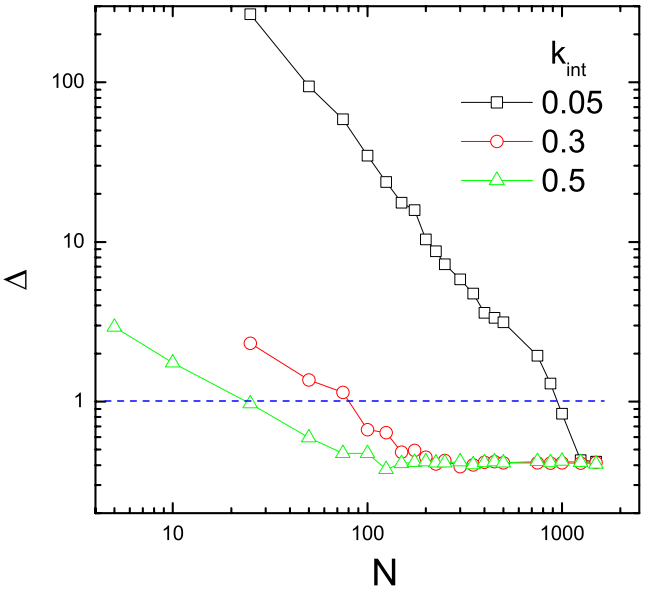

FIG. 5. (Color online) The thermal-diode gain Δ as a function of the system size N for a coupling constant of k_{int}=0.05, 0.3, and 0.5. The dashed blue line indicates the case of Δ=1.

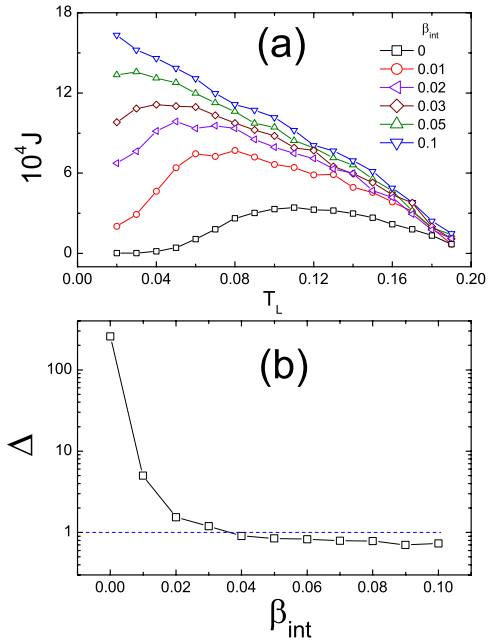

FIG. 6. (Color online) (a) Heat flux as a function of the temperature T_L of the left boundary for various values of the nonlinear coupling constant β_{int}. (b) The thermal-diode gain Δ as a function of the nonlinear coupling constant β_{int}. The dashed blue line indicates the case of Δ=1. The parameter values employed were k_{int} =0.05 and N=25.

It is thus clear that the system will not exhibit NDTR if the coupling between the segments is sufficiently strong or if the system size is sufficiently large. To further study the role of nonlinearity in the exhibition of NDTR, a quartic coupling term was added to the Hamiltonian of the segment interface,

$$H_{int} = \frac{k_{int}}{2}(x_{L,N_L} - x_{R,N_R})^2 + \frac{\beta_{int}}{4}(x_{L,N_L} - x_{R,N_R})^4, \qquad (4)$$

where β_{int} is here referred to as the nonlinear coupling constant. Such addition of a quartic term is a common and simplest way of investigating the role of nonlinearity in the dynamical behavior of a system [9]. Figure 6(a) depicts the heat flux J as a function of the temperature T_L of the left boundary for different values of the nonlinear coupling constant β_{int}. The parameter values k_{int}=0.05 and N=25 were chosen. As shown in Fig. 6(a), the regime of NDTR diminishes as the value of β_{int} increases, which is due to an increase in phonon-band mixing for increasing nonlinearity. In this case, the theory of phonon-band mismatch is not applicable. Figure 6(b) depicts the thermal-diode gain Δ as a function of the nonlinear coupling constant β_{int} for a coupling constant of k_{int}=0.05 and a system size of N=25. The dashed blue line indicates the case of Δ=1. As β_{int} increases, the thermal-diode gain Δ decreases. A comparison with Fig. 6(a) also reveals that the case of Δ=1 coincides with the vanishing of the NDTR regime at a critical nonlinear coupling constant.

IV. PHASE DIAGRAM

The transition from the exhibition to the nonexhibition of NDTR for increasing coupling constant at a given system size or for increasing system size at a given coupling constant can be explained as follows: as the coupling constant increases at a given system size or as the system size increases at a given coupling constant, the phonon bands of the segments are no longer separable; instead, they become "mixed" and form one single band. The theory of phonon-band mismatch for the exhibition of NDTR is no longer valid

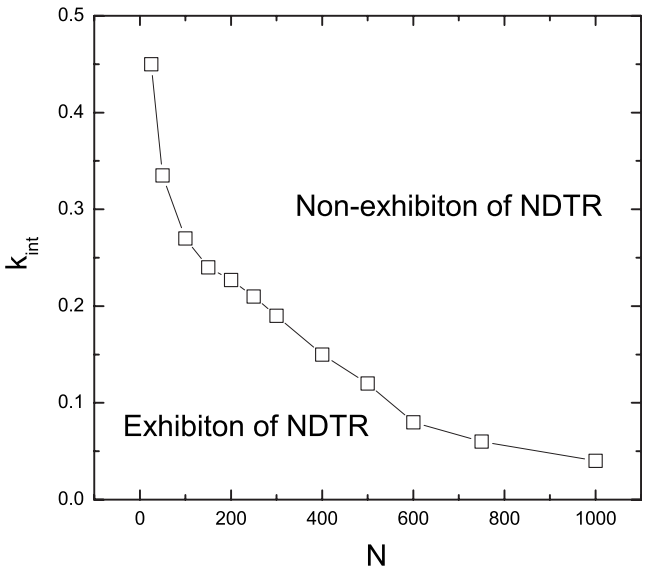

FIG. 7. A "phase" diagram which depicts the range of allowed values of k_{int} and N for the exhibition of NDTR.

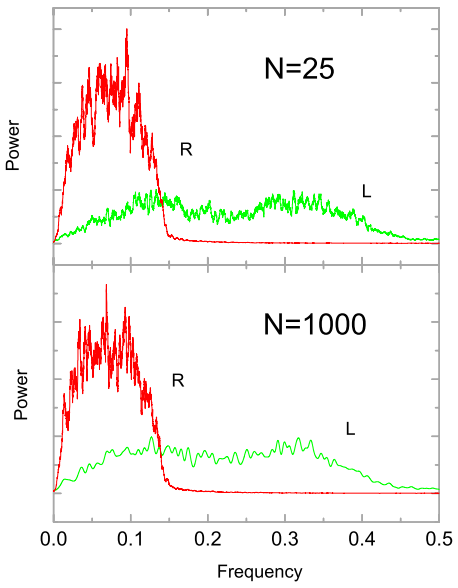

FIG. 8. (Color online) Power spectra of the two particles at the segment interface for two drastically different values of the system size, N=25 and 1000, with the parameter values T_L=0.11, T_R=0.2 and k_{int}=0.05 employed in the simulation. The green (light gray) line is the power spectrum of left particle and the red (heavy gray) line is the power spectrum of right particle. The striking similarity between these two spectra suggests that the conventional power-spectrum explanation of NDTR is not sufficient to account for the transition from the exhibition to the nonexhibition of NDTR for increasing system size.

[9]. A "phase" diagram which depicts the range of allowed values of k_{int} and N for the exhibition of NDTR is shown in Fig. 7. It can be seen that, as the system size increases, the critical coupling constant k_c decreases, and as the coupling constant increases, the critical system size N_c decreases.

V. CONCLUSION

In this paper, the heat-conduction behavior of the one-dimensional two-segment FK model was investigated. It was found that the system exhibits NDTR only if the system size or the coupling constant is sufficiently small. In the existence of a NDTR regime, the link at the segment interface is weak and the corresponding exhibition of NDTR can be explained in terms of effective phonon-band shifts. Figure 8 shows the power spectra of the two particles at the segment interface for two drastically different values of the system size, $N=25$ and 1000. The parameter values $T_L=0.11$ and $T_R=0.2$ with $k_{int}=0.05$ were chosen. The green (light gray) line is the power spectrum of left particle and the red (heavy gray) line is the power spectrum of right particle. It can be seen that the power spectra for these two values of the system size are practically the same, which suggests that the conventional power-spectrum explanation of NDTR is not sufficient to account for the transition from the exhibition to the nonexhibition of NDTR for increasing system size as reported in this paper [13,14]. In fact, there has been evidence that a combination of the self-consistent phonon theory (SCPT) and the Landauer formula is a good candidate for explaining the exhibition of NDTR under the circumstances of a weak intersegment coupling and a small system size. For example, Fig. 3 of Ref. [15] depicts a NDTR regime where the heat flux decreases as the temperature difference increases from −0.7 to −0.4, as obtained by analytical calculations and nonequilibrium molecular dynamics (NEMD) simulations, and the corresponding theoretical analysis was based on the SCPT and the Landauer formula. A recent NDTR study by He *et al.* [22] on the weakly coupled one-dimensional two-segment ϕ^4 model was also based on this theoretical approach. As to practical implications, the operational principles of current models of thermal transistors and thermal logic gates are fundamentally based on the concept of NDTR. This study shows that the exhibition of NDTR depends critically on the properties of segment interfaces. It is therefore believed that the real fabrication of thermal transistors and thermal logic gates would require extra efforts [23] to control the relevant interfacial properties to a sufficiently high precision.

ACKNOWLEDGMENTS

The authors would like to acknowledge members of the Centre for Nonlinear Studies, Hong Kong Baptist University for fruitful discussions. This work was supported in part by the Hong Kong Research Grants Council and the Hong Kong Baptist University. Lei Yang would like to acknowledge financial support from (i) the "100-Person Project" of the Chinese Academy of Sciences and (ii) a China National Natural Science Foundation research grant (Grant No. 10775157).

[1] H. Eisele and G. I. Haddad, in *Modern Semiconductor Device Physics*, edited by S. M. Sze (Wiley, New York, 1998), p. 343.
[2] F. Bonetto, J. L. Lebowitz, and L. Rey-Bellet, in *Mathematical Physics 2000*, edited by A. Fokas, A. Grigoryan, T. Kibble, and B. Zegarlinsky (Imperial College Press, London, 2000), pp. 128–150.
[3] S. Lepri, R. Livi, and A. Politi, Phys. Rep. **377**, 1 (2003).
[4] M. Terraneo, M. Peyrard, and G. Casati, Phys. Rev. Lett. **88**, 094302 (2002).
[5] B. Li, L. Wang, and G. Casati, Phys. Rev. Lett. **93**, 184301 (2004).
[6] B. Li, J. H. Lan, and L. Wang, Phys. Rev. Lett. **95**, 104302 (2005).
[7] J. Lan and B. Li, Phys. Rev. B **74**, 214305 (2006).
[8] D. Segal and A. Nitzan, Phys. Rev. Lett. **94**, 034301 (2005).
[9] B. Hu, L. Yang, and Y. Zhang, Phys. Rev. Lett. **97**, 124302 (2006).
[10] B. Hu and L. Yang, Chaos **15**, 015119 (2005).
[11] B. Hu, D. He, L. Yang, and Y. Zhang, Phys. Rev. E **74**, 060201(R) (2006).
[12] G. Casati, C. Mejía-Monasterio, and T. Prosen, Phys. Rev. Lett. **98**, 104302 (2007).
[13] B. Li, L. Wang, and G. Casati, Appl. Phys. Lett. **88**, 143501 (2006).
[14] N. Yang, N. Li, L. Wang, and B. Li, Phys. Rev. B **76**, 020301(R) (2007).
[15] B. Hu, D. He, L. Yang, and Y. Zhang, Phys. Rev. E **74**, 060101(R) (2006).
[16] L. Wang and B. Li, Phys. Rev. Lett. **99**, 177208 (2007); **101**, 267203 (2008).
[17] V. L. Pokrovsky and A. L. Talapov, *Theory of Incommensurate Crystals*, Soviet Scientific Reviews Supplement Series Vol. 1 (Harwood, New York, 1984).
[18] O. M. Braun and Y. S. Kivshar, Phys. Rep. **306**, 1 (1998).
[19] R. Besseling, R. Niggebrugge, and P. H. Kes, Phys. Rev. Lett. **82**, 3144 (1999).
[20] S. C. Erwin, A. A. Baski, L. J. Whitman, and R. E. Rudd, Phys. Rev. Lett. **83**, 1818 (1999).
[21] B. Hu, B. Li, and H. Zhao, Phys. Rev. E **57**, 2992 (1998).
[22] D. He, S. Buyukdahli, and B. Hu (unpublished).
[23] E. T. Swartz and R. O. Pohl, Rev. Mod. Phys. **61**, 605 (1989).